Available online at www.sciencedirect.com
ScienceDirect
Journal of the Mechanics and Physics of Solids
55 (2007) 788–802

JOURNAL OF THE MECHANICS AND PHYSICS OF SOLIDS

www.elsevier.com/locate/jmps

Yield stress strengthening in ultrafine-grained metals: A two-dimensional simulation of dislocation dynamics

S. Lefebvre[a,b], B. Devincre[c], T. Hoc[a,*]

[a]*Laboratoire MSSMAT, UMR 8579 CNRS, Ecole Centrale Paris, Grande Voie des Vignes, 92295 Chatenay-Malabry Cedex, France*
[b]*Altissemiconductor, 91105 Corbeil Essonnes, France*
[c]*Laboratoire d'Etude des Microstructure, UMR104, CNRS-ONERA, 29 Av. de la Division Leclerc, 92322 Chatillon Cedex, France*

Received 26 May 2006; received in revised form 28 September 2006; accepted 3 October 2006

Abstract

The effect of grain size on the tensile plastic deformation of ultrafine-grained copper polycrystals is investigated using a two-dimensional simulation of dislocation dynamics. Emphasis is put on the elementary mechanisms governing the yield stress in multislip conditions. Whatever the grain size, the yield stress is found to follow a Hall–Petch law. However, the elementary mechanism controlling slip transmission through the grain boundaries at yield is observed to change with the grain size. For the larger grain sizes, the stress concentrations due to dislocations piled-up at grain boundaries are responsible for the activation of plastic activity in the poorly stressed grains. For the smaller grain sizes, the pile-ups contain less dislocations and are less numerous, but the strain incompatibilities between grains become significant. They induce high internal stresses and favor multislip conditions in all grains. Based on these results, simple interpretations are proposed for the strengthening of the yield stress in ultrafine grained metals.

Keywords: Plastic deformation; Dislocation dynamics; Size effects; Simulation; Semiconductor material

*Corresponding author. Tel.: +33 1 41 13 16 16; fax: +33 1 41 13 15 63.
E-mail address: thierry.hoc@ecp.fr (T. Hoc).

0022-5096/$ - see front matter © 2006 Elsevier Ltd. All rights reserved.
doi:10.1016/j.jmps.2006.10.002

1. Introduction

In the semiconductor industry, the Moore's law, which predicts a fast increase of the number of components in parallel with a decrease of the integrated circuits cost, entails extensive miniaturization. As a consequence, the interconnects which link all components are continuously reduced in size and new reliability issues are appearing. The mechanical properties of small metallic designs with ultrafine-grained microstructures are, therefore, a key issue and the properties of copper polycrystals with average grain sizes between 200 nm and a few micrometers are currently the object of intensive investigations.

The most important mechanical property of crystals with ultrafine grains is an increase of the yield stress. More precisely, it is experimentally observed that the yield stress increases linearly with the inverse of the square root of the grain size. This well-known relationship is usually referred to under the name of the "Hall–Petch law":

$$\sigma = \sigma_0 + k_{\mathrm{HP}}\, d^{-1/2}, \tag{1}$$

where d is the average diameter of the grains, k_{HP}, the Hall–Petch constant, which is a material property, and σ_0 ideally is the yield stress of the single crystal. In the case of copper, the constant was measured with a good accuracy and $k_{\mathrm{HP}} = 0.11-0.14\,\mathrm{MPa\,m^{1/2}}$ (Hansen and Ralph, 1982; Nieman et al., 1992; Sanders et al., 1997; Hansen, 2004).

Although Eq. (1) provides a realistic prediction for the yield stress of copper polycrystals from large grain sizes down to 1 μm or less, the physical mechanisms underlying this size effect are still a matter of debate.

To summarize, there are two groups of competing models. A first group is based on the concept of dislocation pile-ups formed at grain boundaries (GBs) and assumes that the stress concentrations associated with pile-ups control the slip transfer between grains (Eshelby et al., 1951; Cottrell, 1958; Li, 1963). The other group of models is more consistent with existing work hardening theories and accounts for the formation of slip gradients and the accumulation of dislocations in the vicinity of GBs (Conrad, 1963; Ashby, 1970; Kocks, 1970; Embury, 1971; Hirth, 1972).

When the characteristic length scale of the microstructures become smaller than typically 1 μm, some aspects of the existing continuum models may becomes partly incompatible with experimental observations. This is not the case for dislocation-driven mechanisms that are experimentally seen to be still operative at grain sizes as small as a few nanometers. In contrast, when $d<10\rho^{-1/2}$, where ρ is the dislocation density, multiplication in the bulk should be progressively replaced by dislocation emission at GBs. This transition between multiplication mechanisms in coarse and ultrafine-grained materials was predicted long ago to occur in the micrometer range (Fu et al., 2001; Choi and Suresh, 2002).

Mesoscopic simulations of dislocation dynamics (DD) are well suited to investigations of crystal plasticity in the micrometer range. For example, the Hall–Petch effect was recently studied using two-dimensional (2D) DD simulations. These simulations considered only one active slip system in each grain and evidenced an influence of the nature of the dislocation sources (Biner and Morris, 2002, 2003), as well as that of their density (Balint et al., 2005). Unfortunately, whereas a size effect was reproduced, it was hardly possible to make a clear distinction between Hall–Petch strengthening ($\sigma \propto d^{-1/2}$) and Orowan strengthening ($\sigma \propto d^{-1}$). For this reason, it was assumed in the present work that single slip conditions should not be enforced in the grains of the simulated

polycrystals. Indeed, it is well known that in continuum mechanical terms, the deformation of a polycrystal requires multislip condition in most of the grains in order to maintain the plastic compatibility at GBs (Taylor, 1938; Saada, 2005).

In this paper, we report a first attempt performed with the help of DD simulations to identify the dislocation mechanisms governing the Hall–Petch effect in polycrystals. The grain sizes are in the micrometer range and the grains deform in multiple slip conditions. The objective is to understand which elementary dislocation mechanisms should be accounted for in a physically based model for polycrystal plasticity dedicated to the behavior of interconnects. For this purpose, the "2.5 DD" simulation of Gómez-García et al. (2006)), which mimics three-dimensional (3D) dislocation behavior in 2D, was extended to deal with the properties of dislocations confined inside micrometric grains. The computations were carried out for periodic polycrystals made of 25 square grains and subjected to uniaxial tension. The basic features of the simulations and some modifications are outlined in Section 2. The simulation results are reported in Section 3 and discussed in Section 4.

2. Simulation method

3D simulations of DD are now a robust method for addressing complex problems of crystals plasticity in a predictive manner. However, for numerical reasons, it is practically impossible to compare in 3D dislocation mechanisms occurring at different length scales (e.g., for different grain sizes) without rescaling the dislocation densities. To by-pass this problem, 2D simulations of DD may be of interest (Lépinoux and Kubin, 1987; Ghoniem and Amodeo, 1988; Van der Giessen and Needleman, 1995). The price to pay for the reduction of the dimensionality of dislocations from lines to points is often an oversimplification of the dislocation mechanisms and of the slip geometry. For instance, it is well known that most 2D simulations overestimate the stability of dislocation dipoles and fail to reproduce the formation of junctions at the intersection of glide planes. For this reason, improved models were recently proposed (Gómez-García et al. 2000, 2006; Benzerga et al., 2004). These new simulations, some time referred to as "2.5 D" simulations, incorporate additional constitutive rules to mimic as closely as possible the 3D mechanisms and dynamics of dislocations. In the present work, the 2.5 DD formulation by Gómez-García et al. (2000, 2006)) for the single crystal is extended to treat polycrystal plasticity.

2.1. Simulated microstructure

As schematically shown in Fig. 1, four different slip systems are defined in a simulation plane that is normal to the z reference axis. Four different types of edge dislocations are then defined, of which the respective Burgers vectors also are in the (xy) simulation plane. This allows defining four different Schmid factors with respect to the tensile axis y. For comparison to experiment, the model material is copper, where the magnitude of the Burgers vector is $b = 2.55 \times 10^{-10}$ m. In the assumption of elastic isotropy, the shear modulus is $\mu = 42$ GPa and the Poisson's ratio is $\nu = 0.324$.

The simulated polycrystal is made up of 25 square grains of side d, tiling a square reference simulation cell of linear dimension $L = 5d$. In the present simulation Born-von Karman boundary solution (named in what follows periodic boundary conditions) is used.

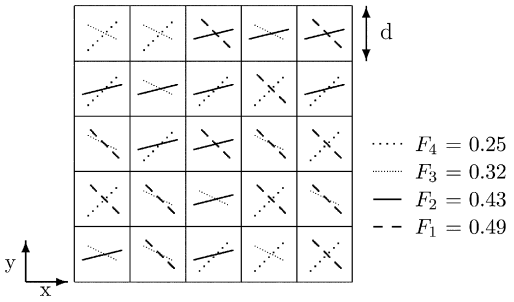

Fig. 1. Sketch of a simulated periodic polycrystal. The simulation cell comprises 25 square grains of linear dimension d. The two slip systems, which are randomly selected in each grain out of four possible slip systems, are schematically shown and the magnitude of the four corresponding Schmid factors is indicated.

Periodic conditions are applied at the boundaries of the primary simulation cell, using a specific procedure that removes artifacts observed in simulations with periodic cells (see Gómez-García et al., 2006 for details). It is worth noting that tests have been performed to check that simulation results are not significantly modified if one uses alternatively 3×3 or 7×7 grains unit cell. Each grain contains two slip systems that are selected at random among four possible ones (see Fig. 1). This defines a combination of two Schmid's factors (F) in each grain and is, therefore, equivalent to setting up the misorientations between the grains. Four different grain sizes are investigated, $d = 0.5$, 0.7, 1 and 2 μm. Each grain initially contains a random distribution of dislocations in density $\rho_0 \approx 10^{13}\,\mathrm{m}^{-2}$.

In agreement with most experimental observations, the GBs are assumed to be impenetrable barriers to dislocation motion (Sutton and Balluffi, 1996). Thus, the dislocations that are blocked at GBs can be viewed as geometrically necessary dislocations accommodating for the plastic strain incompatibilities between grains. In addition, one must notice that the internal stress associated to elastic strain incompatibilities between grains is neglected since linear isotropic elasticity is used.

2.2. Resolution of the dynamics

The procedure used to simulate DD (Ghoniem and Amodeo, 1988; Van der Giessen and Needleman, 1995; Benzerga et al., 2004; Gómez-García et al., 2006) can be summarized as follows. At every time step, (i) a load increment is applied, (ii) the dislocation stress fields and the Peach–Koeler forces are computed at the coordinates of the point-like dislocations, (iii) the displacement of the dislocations is predicted using a stress vs. velocity law and (iv) the possible occurrence of dislocation reactions is examined with the help of local rules.

The resolved effective stress on dislocations, τ^*, is defined by

$$\tau^* = \zeta(\tau_{\mathrm{app}} + \tau_{\mathrm{int}}), \tag{2}$$

where $\tau_{\mathrm{app}} = F\sigma_{\mathrm{app}}$ is the resolved applied stress. This applied stress is assumed to be uniform in the simulated area. τ_{int} is the resolved internal stress. This stress, which is resolved in the dislocation glide plane, is obtained from the sum of all Peach–Koehler interactions with other dislocations in the simulated cell as well as image dislocations located in its periodic replicas (Hirth and Lothe, 1992). This boundary problem, i.e., the

contribution of the periodic external boundaries to the effective stress, is calculated with the help of the fast multipole method (Wang and Lesar, 1995). A phenomenological multiplying factor ζ is introduced in Eq. (2), in order to account for the line tension force that opposes the expansion dislocation loops in 3D. In agreement with early estimates (Saada, 1960), as well as 3D simulations results (Madec et al., 2002), ζ must be of the order of 0.2 to adequately scale down the effective stresses in 2D.

The dislocation mobility law is written:

$$v = \frac{\tau^* b}{B_{Cu}}, \tag{3}$$

where $B_{Cu} = 5.5 \times 10^{-5}$ Pa s is a viscous drag coefficient accounting for the damping of dislocation velocities by electrons and phonons.

The modeling of the reactions between dislocations is based on three local rules (Gómez-García et al., 2000, 2006):

- The annihilation of dislocation with opposite Burgers vectors takes place when their approach distance is less than $5b$.
- In Gómez-García et al. (2006), the possibility of junction formation is tested when two attractive dislocations, gliding in non-parallel slip planes, are reaching approach distances smaller than $\ell_j \approx 0.2\rho^{-1/2}$. The characteristic length ℓ_j is such that it imposes a similar probability for junction formation in 2D and 3D. In the present work, the dislocation densities are similar in all calculations and, for the sake of simplicity, a constant value $\ell_j = 400b$ is used. When a junction is formed, the interaction stress between the two reacting dislocations is set to zero since the two lines are supposed to have merged into a single line.
- Once a junction is formed it remains stable provided that the effective stress on the two interacting dislocations is smaller than a critical destruction stress τ_j given by

$$\tau_j = \beta_j \sqrt{\rho_l}, \tag{4}$$

where ρ_l is a local dislocation density, which is obtained by measuring the radius R_j of a disc centered at the junction and containing 12 dislocations. Hence, $\rho_l = 12/(\pi R_j^2)$. $\beta_j = 0.1$ is a material constant setting the strength of a junction. More detail on the adjustment of this parameter can be found in Gómez-García et al. (2000). Eq. (4) aims at reproducing the physical process of junction unzipping, which is controlled in 3D by the length of the dislocation arms connecting the junctions. This is why τ_j scales with the square root of the local dislocation density.

Finally, it was checked that the results reported in Section 3 are not sensitive to these three local rules, since very few junctions are formed inside the small grains considered in the present study.

Simulated tensile tests are performed by imposing a constant strain rate of $10\,s^{-1}$ in plane strain conditions. With this value of the strain rate, the velocity law entails a negligible strain rate sensitivity in the simulation output.

Dislocation glide is the only deformation mechanism considered and diffusion driven processes like climb or GB sliding are assumed to be negligible. This assumption is well justified at room temperature and with grain dimensions in the micrometer range.

2.3. Dislocation emission

The mobile dislocations that carry the plastic strain rate are produced by two different mechanisms, the relative weight of which depends upon the grain size: dislocation multiplication inside the grains and dislocation emission at or close to GBs. This last process cannot be formally accounted for in mesoscopic simulations, by lack of knowledge of the critical conditions for dislocation emission. In the present case, it is replaced by a local rule, which, in contrast with the one proposed by Gómez-García et al. (2006), is able to generate dislocations at any site in the grains. Thus, it mimics multiplication in the bulk and simultaneously assimilates emission at GBs to dislocation generation close to GBs.

This simulation rule is based on the generation of a pair of dislocations with opposite sign at a certain site. The latter is initially selected at random in the whole simulated area and remains fixed all through the computation. In agreement with experiment, the source density is taken proportional to the surface fraction of GBs (Konopka et al., 2000; Malis and Tangri, 1979). In the present study an average of one source per length 300 nm of 2D grain boundary is imposed. As the source distribution is random, it may happen that no source is found inside the smallest grains. For this reason, at least three calculations starting with different initial configurations have been performed for the smallest grain sizes ($d = 0.5$ and $0.7\,\mu$m). Dislocation emission is conditioned by (i) a critical stress τ_s and (ii) a time interval between two emissions, Δt_s. In earlier studies (Gómez-García et al., 2000) it was found that the activity of this type of sources is well described by

$$\Delta t_s = \frac{5\mu B}{\tau_s^2} \ln\left(\frac{\tau^*}{\tau^* - \tau_s}\right), \tag{5}$$

where τ^* is the effective stress at the position of the generation point. The value of τ_s is arbitrarily set at a rather low value, 16 MPa, and the initial coordinates of the two dislocation emitted at a source are determined using an iterative procedure, which can be summarized as follows:

- Two dislocations of opposite sign are introduced close to each other on each side of the generation point and in the same glide plane (the initial spacing is 10 b).
- The stability of this configuration is checked, that is, the effective stress is computed on the two dislocations to determine their glide directions.
- If the configuration tends to collapse, the spacing between the two dislocations is increased by 10b increments and iterations are performed until an equilibrium position is found. This equilibrium position is obtained in the presence of a small constant friction stress (0.5 MPa). In addition, it must be emphasized that the equilibrium configuration is usually asymmetric with respect to the emission point. Indeed, as soon as one of the two dislocations is in equilibrium or blocked at a GB, only the second dislocation adjusts is position during further iteration.
- Finally, if no expanding configuration is found within 500 iterations, the two dislocations are removed and the source is considered as inactive.

One must notice that the real value of τ_s is defined by the equilibrium configuration and is, therefore, much higher than 16 MPa. This emission procedure allows emitting new dislocations very close or at GBs and also introduces variations of τ_s consistent with experimental evidence (Sutton and Balluffi, 1996; Konopka et al., 2000). Indeed, detailed

investigation of this procedure shows that in average τ_s behaves like $1/r$, where r is the distance from the emission point to the closest GB in the glide plane. This property of sources manifests itself in the simulations through an increase of the emission stress when the grain size decreases.

3. Simulation results

3.1. Size effect

The mechanical response of the polycrystals is illustrated in Figs. 2 and 3 for the four grain sizes used in the present study. Fig. 2 shows the applied stress vs. plastic strain curves. The elastic contributions are removed from this figure to allow comparing these curves. From the evolution of the dislocations during straining, it appears that one can distinguish two different stages on the stress–strain curves. There is first a transient regime, during which plastic deformation mainly results from the motion toward the GBs of the dislocations initially present inside the grains. In the second stage, the strain hardening rate is quasi-constant and plastic deformation arises from new dislocation emission events. The transition between these two regimes occurs around a plastic strain that is very small, $\varepsilon_p \approx 0.03\%$, and at a stress such that the dislocation emission sites start becoming active. In what follows, the yield stress of the ultrafine-grained polycrystals is assimilated to the proof stress at a plastic strain $\varepsilon_p = 0.1\%$.

Irrespective of the strain value, the flow stress significantly increases with decreasing grains size. To quantitatively assess this size effect, the yield stress is plotted in Fig. 3 as a function of d on a Log–Log scale. This plot clearly emphasizes that the simulation results fit well a $d^{-1/2}$ scaling law. From Eq. (1) and setting a conventional value of $\sigma_0 = 20\,\text{MPa}$, a linear regression analysis yields a Hall–Petch constant $k_{HP} = 0.23\,\text{MPa}\,\text{m}^{1/2}$ with a high correlation coefficient ($r^2 = 0.98$). It is worth noting that this calculation is weakly sensitive

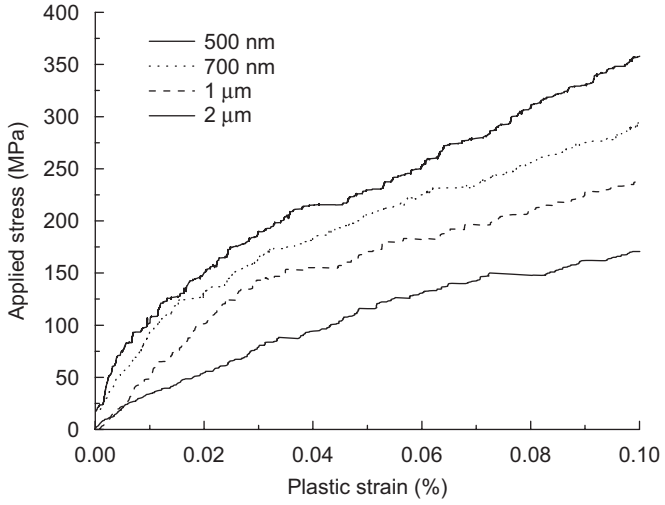

Fig. 2. Plot of the applied stress, σ_{app}, vs. the plastic strain ε, for the four simulated polycrystals. The grain sizes are indicated.

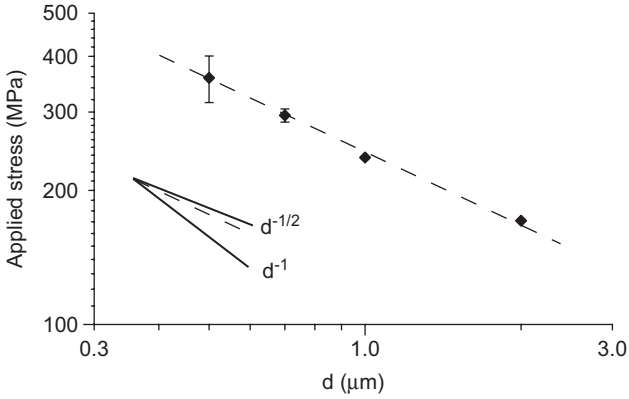

Fig. 3. Plot of the applied stress, σ_{app}, determined at a plastic strain of 0.1% vs. d, where d is the grain size, for the four simulated polycrystals. Error bars on σ_{app} are given for small grains. A dashed line going through the simulation results is shown as a guide to eye and for comparison with the slopes $d^{-1/2}$ and d^{-1}.

to the magnitude of σ_0. This result is consistent with experiments on ultrafine grained copper polycrystals (Espinosa et al., 2004; Sanders et al., 1997; Huang and Hansen, 2004), as well as aluminum and iron polycrystals (Tsuji et al., 2002). In contrast, an Orowan fit of the stress vs. d^{-1} yields $\sigma = 20 + 1.9 \times 10^{-4} d^{-1}$ with a correlation coefficient of only $r^2 = 0.6$. Hence, one can conclude that a Hall–Petch effect is well reproduced in polycrystals with grain sizes in the micrometer range.

3.2. Dislocation microstructures

The dislocation microstructures obtained at $\varepsilon_p = 0.1\%$ are shown in Fig. 4 for two different grain sizes, $d = 500$ nm and $d = 2\,\mu$m. They consist of individual dislocations and dislocation pile-ups at GBs. An analysis of the spatial distribution of the dislocation reveals that the dislocation density blocked at or near GBs increases when the grain size decreases, from 65% for the 2 μm grains to 80% for the 500 nm grains. This result is in good agreement with the observation that no dislocation is found inside the grains volume of ultrafine grained polycrystals (Kumar et al., 2003).

In addition, a monitoring of the emission rate during simulations shows that for the smaller grain sizes, the fraction of active sources increases, from only 28% for 2 μm grains to 42% for 500 nm grains. This trend must be related to the observation that, for a given plastic strain, the dislocation pile-ups are less numerous and contain a smaller number of dislocations with decreasing grain sizes.

A comparison between Figs. 4a and b, where one grain in the former is as large as 16 grains in the latter, suggests that the dislocation density increases faster in polycrystals with smaller grains. A measurement of the total dislocation density in the simulated polycrystal shows that it increases linearly with strain and decreases like the inverse of the grain size, as illustrated in Fig. 5. A linear regression analysis yields a very high correlation coefficient of $r^2 = 0.98$. Thus, one can write

$$\frac{d\rho}{d\varepsilon_p} = \frac{5}{bd}. \tag{6}$$

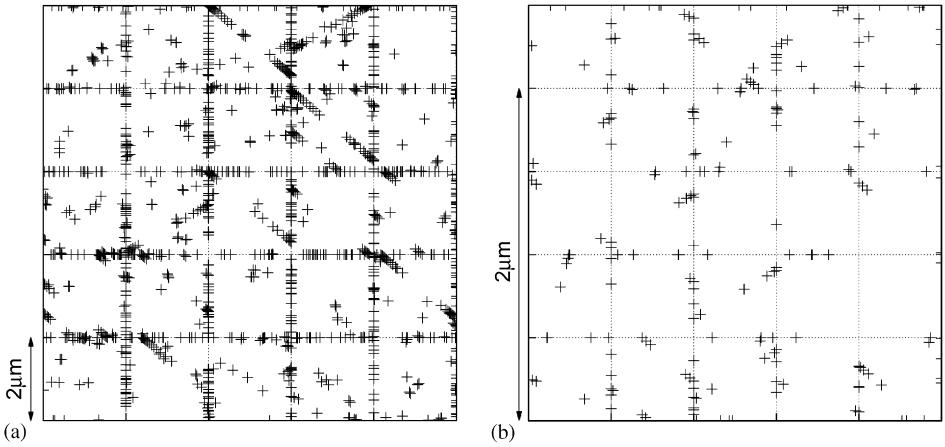

Fig. 4. Dislocation microstructures at $\varepsilon_p = 0.1\%$ for polycrystals with grain size $d = 2\,\mu m$ (a) and $d = 500\,nm$ (b).

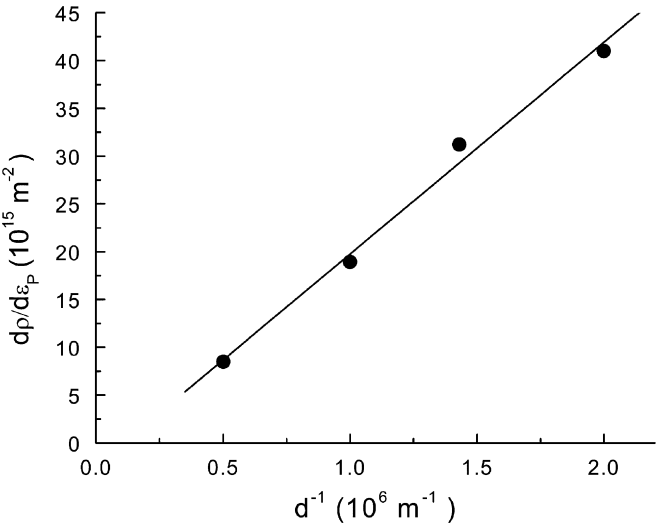

Fig. 5. Rate of increase of the dislocation density vs. d^{-1} for the four simulated polycrystals. The linear regression line has a correlation coefficient $r^2 = 0.98$.

This relation can be viewed as expressing a storage rate, which, as expected from a storage-recovery model, is governed by a dislocation mean free path $\Lambda = d$ (Embury, 1971).

3.3. Slip systems and local stresses

To correlate the dislocation microstructures to the local stresses in the grains, the active slip systems were analyzed in a first step. The contribution of each of the four possible slip systems to the plastic strain in the whole simulated polycrystal was monitored. This

contribution is found to depend on the grain size. In the polycrystal with $d = 2\,\mu m$, the slip system with the highest Schmid's factor ($F = 0.49$) is four times more active than the three others. Hence, in this case, the grain orientation is still controlling plasticity at small strains. The situation is quite different in the polycrystal with the smallest grain size. In the latter case the plastic strain is almost uniformly distributed among the four slip systems. This homogenization of deformation indicates that the slip activity inside grains is not governed any more by the Schmid's law.

Local stresses were examined in order to further investigate the homogenization of plastic strain that is found for small grain sizes. For this purpose, mappings of the dislocation stress fields were computed on a grid containing of 100×100 measurement points tiling the total simulated area. Two representative scalar stresses were then computed. The first one is the component of the internal stress tensor along the direction of the applied stress σ_{yy}. The second one is the von Mises stress which provides an information on the magnitude of the local stress. It is defined by

$$\sigma_Y^2 = \tfrac{1}{2}[(\sigma_{xx} - \sigma_{yy})^2 + (\sigma_{yy} - \sigma_{zz})^2 + (\sigma_{zz} - \sigma_{xx})^2 + 6(\sigma_{xy}^2)]. \tag{7}$$

This stress was computed at the yield point.

As illustrated in Fig. 6a, the von Mises stress computed from the dislocation fields clearly images strong internal stress concentrations at the GBs of the polycrystal with the largest grain size.

This result could have been anticipated since it reflects the accumulation of dislocations at or near GBs or, equivalently, the existence of plastic strain incompatibilities between grains. More interesting is the mapping of σ_Y for the polycrystals with smaller grains (Fig. 6b). In that case, the von Mises stress is much more heterogeneous and exhibits areas with large local stresses inside the grains. Hence, the difference between the boundaries and the volume of the grains becomes less marked than in Fig. 6a. This change results from the long-range nature of the dislocation stress fields. Indeed, when the grain size decreases, the highly stressed area fraction of the grain containing dislocations blocked at or near GBs

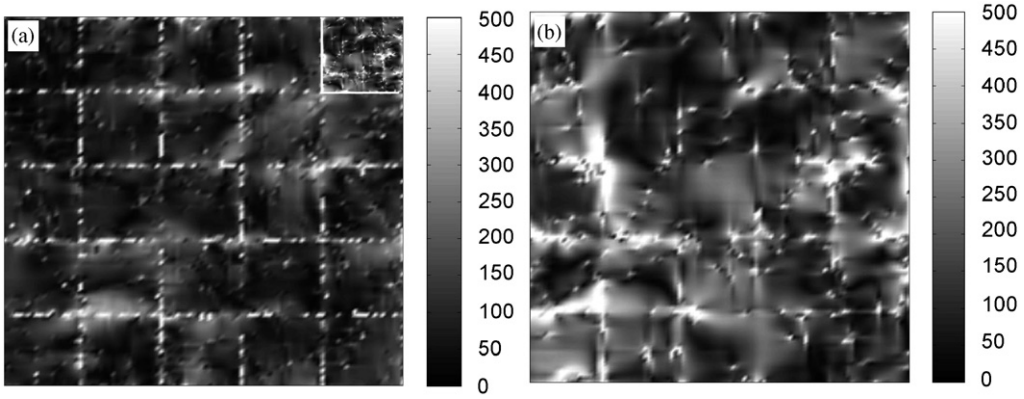

Fig. 6. Mappings of the von Mises stress σ_Y, in MPa, in two strained polycrystals with grain sizes $d = 2\,\mu m$ (a) and $d = 500\,nm$ (b) and at a plastic strain $\varepsilon_p = 0.1\%$. The applied stress is 171 MPa in (a) and 338 MPa in (b). The stress values, in MPa, are coded in gray levels. To allow comparing the two spatial distributions of stresses, a mapping for 16 grains of (b) is shown in the upper right corner of (a).

increases. In parallel, the number of dislocation sources per unit volume is also increasing, since it is indexed to the total length of GBs. These two factors contribute to the activation of slip systems with low Schmid's factors and to the homogenization of the plastic strain. Nevertheless, the maximum internal stresses are still measured in the vicinity of the grains containing the slip system with the highest Schmid's factor. Finally, the mean values of the von Mises stresses computed from Fig. 6a and b are also reflecting the size effect found on the stress–strain curves. They are about two times larger for a grain size $d = 500\,\text{nm}$ than for $d = 2\,\mu\text{m}$.

4. Discussion

4.1. The role of dislocation generation

It is instructive to perform a comparison between the present study and previous simulations studies (Biner and Morris, 2002, 2003; Balint et al., 2005) based on similar hypotheses regarding the polycrystal conditions and the DD.

- The study by Balint et al. (2005) shows that a lack of dislocation sources significantly modifies the plastic properties. Here, one finds that the fraction of the available sources that is activated is always below 50%. Thus, one can conclude that the number of emission sites is not a critical simulation parameter provided that it is large enough to be realistic and that multislip conditions are implemented.
- In the work by Biner and Morris (2002, 2003), the key parameter for reproducing an Hall–Petch effect is taken to be the critical stress for dislocation generation and not the position or density of the dislocation emission sites. Here, no preset critical stress is defined and no assumption is made upon the geometry or the dimension of the generation sites. Dislocation emission is assumed to take place as soon as the local conditions favor stress relaxation by plastic activity. These simple conditions, are sufficient for reproducing an increase of the critical generation stress with decreasing grain size (see Fig. 2). Moreover, in such conditions, the detailed properties of the mechanisms that generate dislocations have no significant influence on the mechanical response.

In the present simulation, the key factor is the density of dislocations in the vicinity of the emission sites or, in other words, the internal stress associated to plastic strain incompatibilities between neighboring grains.

4.2. Evolution of the dislocation microstructures

In all simulations, dislocations accumulate at GBs, but the dislocation arrangement significantly evolves with the grain size. A gradual transition is found at yield between microstructures typical of large grain sizes and microstructures that seem to characterize sub-micronic grain sizes. It seems that such a transition has never been reported till now in the literature. From an experimental viewpoint, this is probably because the dislocations microstructures are difficult to observe under load, whereas, upon unloading, the reverse motion of dislocations should induce an annihilation of most of the dislocations stored at GBs.

With decreasing grain sizes, the density of dislocations emitted at sources and blocked at GBs tends to become larger and less and less pile-ups are observed. This effect can be understood as follows. In the smaller grains, a freshly emitted dislocation produces less plastic strain and more dislocations have to be generated per unit volume to carry out the imposed strain rate. Simultaneously, the reduction in grain size increases the back stress from the stored dislocations at the emission points. Hence, the stress needed to generate successive dislocations from a given source increases rather fast. This explains why the formation of dislocation pile-ups becomes difficult in the smaller grains (cf. Section 2.1). As a consequence, the activation of many sources emitting less dislocations is favored, including in slip systems with a small Schmid factor.

The consideration of slip activity as a result of internal stresses at the dislocation generation sites can be extended to the interactions between grains. In the small grains, the dislocations blocked at the boundaries of a plastically deformed grain are, in average, closer to the active generation sites in the neighboring grain. In the latter, this also enhances slip activity on the slip systems with low Schmid factors. Thus, the decrease of the distance between generation sites and GBs with decreasing grain sizes promotes significant effects related to the increased internal stresses at the emission sites.

To check this last effect, the internal stress parallel to the loading axis can be split in two contributions. The first contribution, σ^G_{yy}, arises from dislocations located inside the grain in which the stress is measured, whereas the second contribution, σ^E_{yy}, is due to dislocations located in other grains. A detailed analysis of these two contributions shows that σ^G_{yy} continuously decreases with increasing grain size. The behavior of σ^E_{yy} is quite different, as illustrated by Fig. 7. In the polycrystals with the largest grain size (Fig. 7a) σ^E_{yy} is quite small in comparison to the applied stress and the "local" contribution σ^G_{yy}. Only a few sites of high stress concentrations are found near the tip of pile-ups in adjacent grains (compare with Fig. 4a). In polycrystals with smaller grain sizes (Fig. 7b), the contribution of σ^E_{yy} to the total stress is much more substantial. Moreover, the absolute values of σ^E_{yy} and σ^G_{yy} are comparable in all grains. This explains the uniformity of plastic strain recorded for small grain sizes (cf. Section 2.1).

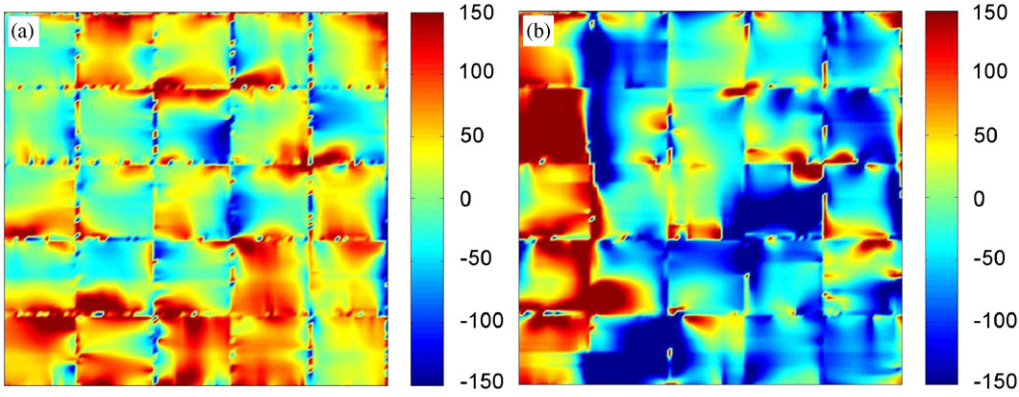

Fig. 7. Mappings of the axial internal stress σ^E_{yy} in MPa, due to dislocations located outside the considered grain. This stress is computed at a strain $\varepsilon_p = 0.1\%$. The grain size is $d = 2\,\mu m$ in (a) and $d = 500\,nm$ in (b). The stress values, in MPa, are coded in gray levels.

4.3. The Hall–Petch relation

As could be expected, the decrease in grain size governs yield strengthening in polycrystals with grains sizes in the submicron range. The smaller is the grain size, the larger is the dislocation density needed to produce plastic strain. In addition, it was shown that in small grains, the emission of dislocations in slip systems with a favorable Schmid factor is rapidly exhausted. This is why the activation of many sources is observed and multiple slip is rapidly activated inside the grains.

The linear dependence of the dislocation density on strain found in the simulations (Eq. 6) can easily be explained in terms of a storage rate (Ashby, 1970; Kocks, 1970; Embury, 1971). Each generated dislocation loop produces a shear strain $\Delta\gamma \approx b/d$ in 2D (one can check easily that the same argument is also valid in 3D). Once it is blocked at a GB, the stored dislocation density has increased by $\Delta\rho = 4d/d^3 = 4/d^2$. Thus, one has $\mathrm{d}\rho/\mathrm{d}\varepsilon_\mathrm{p} = \kappa/bd$, in good agreement with Eq. (6), where $\kappa = 5$.

In isotropic elasticity, the differences in elastic deformations between the grains do not generate incompatibility stresses. Thus, the stress incompatibilities are mostly due to plastic strain incompatibilities mediated by the stress fields of the dislocations blocked at boundaries. In this context, the dislocation microstructure of the polycrystal can be assimilated to a kind of Taylor (1934) network and one can write

$$\sigma = M\alpha\mu b\sqrt{\rho}, \tag{8}$$

where α is a constant close to 0.5 and M is the Taylor factor defined by $M = \sum_\mathrm{s} \mathrm{d}\gamma_\mathrm{s}/\mathrm{d}\varepsilon_\mathrm{p}$ and equal to 3.067.

By combining Eq. (8) and the integrated form of Eq. (6), one obtains a simple constitutive relation for the strengthening of polycrystals with grain size in the micrometric range:

$$\sigma \approx \sigma_0(\varepsilon) + M\alpha\mu\sqrt{\frac{5b\varepsilon_\mathrm{p}}{d}}. \tag{9}$$

This simple equation is similar to the result of Embury (1971) and emphasized a possible dependency of σ_0 with ε as discussed in Hirth and Lothe (1992).

For comparison with experiments, when considering $\varepsilon_\mathrm{p} = 0.2\%$, the value of k_HP obtained from this relationship is close to $0.1\,\mathrm{MPa\,m^{1/2}}$. This value is physically meaningful and suggests that the present simulation was successful to capture the critical phenomena at the origin of the Hall–Petch effect.

Eq. (9), is only based on variation of dislocation storage rate when the mean free path of dislocation is altered by GBs. This equation is therefore not microstructural dependent and the microstructure evolution observed in the simulation is not expected to change the Hall–Petch law (see Fig. 3). Microstructure evolution reflects only modifications of dislocation emission and multiplication mechanism in order to satisfy a mechanically required storage rate.

5. Conclusion

The yield stress of polycrystals with grain sizes ranging from 500 nm to 2 μm was investigated with the help of 2.5 DD simulation. At a proof strain $\varepsilon_\mathrm{p} = 0.1\%$, a conventional Hall–Petch type of scaling law was successfully reproduced. The constant of

the Hall–Petch law is found to be $k_{HP} \approx 0.23\,\mathrm{MPa\,m^{-1/2}}$, that is twice the experimental value measured for bulk copper polycrystals. This overestimate of k_{HP} may arise from the small number of slip systems available in the simulated grains. Indeed, it is well know that the yield stress of a crystal is related to the number of active slip systems. Unfortunately, incorporating more slip systems in a computer model based on densities of infinitely parallel dislocations does not necessarily make it more realistic.

The present work constitutes a first attempt to identify the dislocation mechanisms controlling the size effect in ultrafine-grained polycrystals in multiple slip conditions. It suggests that even if the yield stress follows the Hall–Petch law for grain sizes ranging from 2 μm down to 500 nm, the elementary mechanisms involved are different. In submicron grained polycrystals, stress concentrators like dislocation pile-ups are no longer needed for transmitting plastic strain through the grains. Indeed, the deformation of each grain promotes large plastic strain incompatibilities which, in their turn, induce a homogeneous distribution of plastic strain in the grains. Thus, the mechanisms of yield strengthening in ultrafine-grained polycrystals looks simpler than in conventional polycrystals.

The simulation results confirm that one can use in ultra fine polycrystal the classical strengthening models based on the dislocation mean free path. Work is in progress to generalize the scalar Hall–Petch constitutive relation discussed above and utilize it in a finite element code for crystal plasticity. This would allow making critical comparisons between modeling and experiment.

Acknowledgments

Discussions with L. Kubin and P. Vekeman were very helpful. Support from Altissemiconductor is gratefully acknowledged.

References

Ashby, M., 1970. The deformation of plastically non-homogeneous materials. Philos. Mag. 21, 324–399.

Balint, D., Deshpande, V., Needleman, A., Van der Giessen, E., 2005. A discrete dislocation plasticity analysis of grain-size strengthening. Mater. Sci. Eng. A 400–401, 186–190.

Benzerga, A., Bréchet, Y., Needleman, A., Van der Giessen, E., 2004. Incorporating three-dimensional mechanisms into two-dimensional dislocation dynamics. Model. Simul. Mater. Sci. Eng. 12, 159–196.

Biner, S., Morris, J., 2002. A 2D discrete dislocation simulation of the effect of grain size on strengthening behaviour. Model. Simul. Mater Sci. Eng. 10, 617–635.

Biner, S., Morris, J., 2003. The effects of grain size and dislocation source density on the strengthening behaviour of polycrystals: a 2D discrete dislocation simulation. Philos. Mag. 83 (31–34), 3677–3690.

Choi, Y., Suresh, S., 2002. Size effects on the mechanical properties of thin polycrystalline metal films on substrates. Acta Mater 50, 1881–1893.

Conrad, H., 1963. Effect of grain size on the lower yield and flow stress of iron and steel. Acta Metall. 11, 75–77.

Cottrell, A., 1958. Theory of brittle fracture in stell and similar metals. Trans. Metal. Soc. AIME 212, 192–203.

Embury, J., 1971. Strengthening Methods in Crystals. Elsevier, Amsterdam, p. 331.

Eshelby, J., Frank, F., Nabarro, F.R.N., 1951. The equilibrium of linear arrays of dislocations. Philos. Mag. 42, 351–364.

Espinosa, H., Prorok, B., Peng, B., 2004. Plasticity size effects in free-standing submicron polycrystalline fcc films subjected to pure tension. J. Mech. Phys. Solids 52, 667–689.

Fu, H.-H., Benson, D., Meyers, M., 2001. Analytical and computational description of effect of grain size on yield stress of metals. Acta Mater 49, 2567–2582.

Ghoniem, N., Amodeo, R., 1988. Computer simulation of dislocation pattern formation. Solid State Phenom. 3–4, 377–388.

Gómez-García, D., Devincre, B., Kubin, L.P., 2000. Forest hardening and boundary conditions in 2D simulations of dislocations dynamics, in: Robertson, I.M., Lassila, D.H., Devincre, B., Phillips, R. (Ed.), Multiscale Phenomena in Materials—Experiments and Modeling. vol. 578. MRS, Warrendale, Pennsylvania, pp. 131–136.

Gómez-García, D., Devincre, B., Kubin, L., 2006. Dislocation patterns and the similitude principle: 2.5D mesoscale simulations. Phys. Rev. Lett. 96, 125503, (1–4).

Hansen, N., 2004. Hall–Petch relation and boundary strengthening. Scripta Mater. 51, 801–806.

Hansen, N., Ralph, B., 1982. The strain and grain size dependence of the follow stress of copper. Acta Metall. 30, 411–417.

Hirth, J., 1972. The influence of grain boundaries on mechanical properties. Metall. Trans. 3, 3047–3067.

Hirth, J.P., Lothe, J., 1992. Theory of Dislocations. Krieger, Malabar, Florida.

Huang, X., Hansen, N., 2004. Mater. Sci. Eng. A 387–389, 186–190.

Kocks, U., 1970. The relation between polycrystal deformation and single crystal deformation. Metall. Trans. 1, 1121–1143.

Konopka, K., Mizera, J., Wyrzykowski, J., 2000. The generation of dislocation from twin boundaries and its effects upon the flow stress in fcc metals. J. Mat. Proces. Technol. 99, 255–259.

Kumar, K., Van Swygenhoven, H., Suresh, S., 2003. Mechanical behavior of nanocrystalline metals and alloys. Acta Mater. 51, 5743–5774.

Lépinoux, J., Kubin, L.P., 1987. The dynamic organization of dislocation structures: a simulation. Scripta Metall. 21, 833–838.

Li, J., 1963. Petch relation and grain boundary sources. Trans. Metal. Soc. AIME 277, 239–247.

Madec, R., Devincre, B., Kubin, L., 2002. From dislocation junctions to forest hardening. Phys. Rev. Lett. 89, 255508, (1–4).

Malis, T., Tangri, K., 1979. Grain boundaries as dislocation sources in the premacroyield strain region. Acta metall. 27, 25–32.

Nieman, G., Weertman, J.R., Siegel, R., 1992. Mechanical behavior of nanocrystalline metals. Nanostr. Mater 1, 185–190.

Saada, G., 1960. Sur le durcissement dû à la recombinaison des dislocations. Acta Metall. 8, 841–847.

Saada, G., 2005. From single crystal to the nanocrystal. Philos. Mag. 85, 3003–3018.

Sanders, P., Youngdahl, C., Weertman, J.R., 1997. The strength of nanocrystalline metals with and without flaws. Mater. Sci. Eng. A 234–236, 77–82.

Sutton, A., Balluffi, R., 1996. Interfaces in Crystalline Materials. Monographs on the Physics and Chemistry of Materials. Clarendon Press, Oxford.

Taylor, G., 1934. The mechanism of plastic deformation of crystals. Part I.—Theoretical. Proc. R. Soc. London, 362–387.

Taylor, G., 1938. Plastic strain in metals. J. Inst. Metals 62, 307.

Tsuji, N., Yto, Y., Saito, Y., Minamino, Y., 2002. Strength and ductility of ultrafine grained aluminum and iron produced by ARB and annealing. Scripta Mater. 47, 893–899.

Van der Giessen, E., Needleman, A., 1995. Discrete dislocation plasticity: a simple planar model. Model. Simul. Mater. Sci. Eng. 3, 689–735.

Wang, H.Y., Lesar, R., 1995. O(n) algorithm for dislocation dynamics. Philos. Mag. A 71, 149–164.